Research Square

Preprints are preliminary reports that have not undergone peer review.
They should not be considered conclusive, used to inform clinical practice,
or referenced by the media as validated information.

Phenotypic characteristics distinguishing bloodstream form and central nervous form of *Trypanosoma brucei rhodesiense.*

Kariuki Ndung'u (kariukindungu1960@gmail.com)
Kenya Agricultural and Livestock Research Organization-Biotechnology Research Insstitute
Grace Adira Murilla
KAG EAST University
John Kibuthu Thuita
Meru University of Science and Technology
John Maina Kagira
Jomo Kenyatta University of Agriculture and Technology
Paul O. Mireji
Kenya Agricultural and Livestock Research Organization
Geoffry Njuguna Ngae
Kenya Agricultural and Livestock Research Organization
Purity Kaari Gitonga
Kenya Agricultural and Livestock Research Organization
Samuel Onyoyo Guya
Kenya Agricultural and Livestock Research Organization
Joanna Eseri Auma
Kenya Agricultural and Livestock Research Organization
Paul Onyango Okumu
University of Nairobi
Raymond Ellie Mdachi
Kenya Agricultural and Livestock Research Organization

Research

Keywords: Trypanosoma brucei rhodesiense, blood stream form (BSF), central nervous system (CNS), pathogenicity, characterization

Posted Date: January 24th, 2020

DOI: https://doi.org/10.21203/rs.2.21779/v1

License: This work is licensed under a Creative Commons Attribution 4.0 International License.
Read Full License

Abstract

Background: Phenotypic and morphological characteristics distinguishing from bloodstream form (BSF) and central nervous system (CNS) of *Trypanosoma brucei rhodesiense* (*Tbr*) are poorly understood.

Method: To identify these distinguishing characteristics, we separately infected four donor mice with each of five *Tbr* isolates (KETRI 2537/3537/2656/3459 and EATRO 2291). At 21 days post infection (DPI), donor mice were euthanized, BSF or CNS derived trypanosomes recovered and used for the following studies: 1) determination of morphological characteristics 2) pathogenicity studies using groups of 10 mice per isolate form. We then assessed differences in their lengths and morphology) and other characteristics including pre-patent period (PP), parasitaemia progression, packed cell volume (PCV), body weight, survival times, gross pathology, and histopathology. All analyses of data were conducted using GenStat, UK where $p \leqslant 0.05$ were considered statistically significant. Differences between and within the means were analyzed using one-way ANOVA. General Linear Model was used to analyze data on the length of the trypanosome. Survival data analysis was carried out employing the Kaplan–Meier method. **Results:** Morphologically, the CNS forms were predominantly long slender (LS) while BSF forms consisted of a mixture of short stumpy and intermediate forms. The mean length of CNS trypanosomes was 0.6 micrometer longer than their counterpart BSF derived trypanosomes. The PP was significantly ($p<0.05$) shorter and progression to peak parasitaemia faster (7 vs 9 days) in CNS than BSF derived trypanosomes. PCV declined by 21.6% and 26.9% in BSF and CNS infected mice respectively whereas non-infected control increased by 3.8% at 14 DPI. Body weight changes in BSF and CNS infected mice were (12.7% and 9.2% respectively) and significantly ($p <0.05$) lower than in non-infected control (27.6%) at 14 DPI. Gross pathology changes (splenomegaly and hepatomegaly) and histopathology changes were pronounced in mice infected with CNS relative to BSF trypanosome forms. Changes in histopathology included congestion, infiltration with inflammatory cells, hemolysis and necrosis, all indicators of differential virulence of the forms.

Conclusion: Our study identified higher pathogenicity in CNS relative to BFS derived trypanosome forms in the mouse model. We also identified KETRI 2656 as a suitable isolate for acute menigo- encephalitic studies.

Introduction

Human African Trypanosomiasis (HAT, sleeping sickness) is caused by Trypanosoma brucei rhodesiense (Tbr) and T. b. gambiense (Tbg) species of trypanosomes which are transmitted by tsetse flies of Glossina species [1]. The Tbr is predominant in eastern and southern Africa and causes the acute form while Tbg is predominant in Central and Western Africa and is responsible for the chronic form of HAT [2]. Recognized stages in the clinical presentation of HAT are the hemolymphatic (early) and encephalitic (late) stages that typically manifest as blood Stream form (BSF) and central nervous system, (CNS) forms respectively. The early stage infection is clinically non-specific, manifesting as malaise, headache, arthralgia, generalized weakness, weight loss and anaemia [3]. On the other hand, late stage infection,

occasioned by the parasites crossing the blood-brain barrier or blood- cerebrospinal fluid (CSF) barrier and invading the CNS [4, 5] clinically manifest as psychiatric, motor, sensory and sleep abnormalities[6].The CNS invasion may be aided by parasite and/or host derived factors [5].

In the CNS, the parasites DNA can be detected as early as six days post infection (DPI) in their replicative slender forms[7, 8], with peak infection at 21 DPI [8]. With progression of CNS HAT, changes occur in the cerebrospinal fluid characterized by presence of cytotoxic compounds and reduced cerebrospinal fluid as well glucose levels[9, 10], making it more 'hostile' to the trypanosomes [11, 12]. This is further contributed by the CNS immune response[13]. Phenotypic effects of these factors on CNS recovered/derived-trypanosomes are poorly understood. To investigate effect of these factors on trypanosomes, we hypothesized that there are distinct morphologic and phenotypic differences between the BSF and CNS forms of T.b. rhodesiense trypanosomes that differentially influence the pathogenicity of either form. We thus compared morphologic and phenotypic changes associated with BSF and CNS derived trypanosomes directly harvested from the blood and the brain, respectively, and evaluated their pathogenicity.

Materials And Methods

Ethics

Approval for performing our experiments on mice was obtained from the Kenya Agricultural and Livestock Research Organization -Biotechnology Research Institute - (KALRO- BioRI) Review Board (C/Biori/4/325/II/49) and the protocol reviewed by and approved by the BioRI-KALRO Institutional Animal Care and Use Committee (IACUC).

Selection Of Trypanosomes Isolates

Five Tbr isolates were used in this study (Table 1). They were selected from BioRI (formerly KETRI) cryo-bank and were originally isolated from HAT patients in the three east African countries [14].The isolates had gone between1-8 eight passages in mice. Old and recent isolates were selected for this study.

Table 1
Isolates of T.b. rhodesiense collected from different parts of eastern Africa

Stabilate No:	Locality	Year of isolation	Host of isolation	Passage No
KETRI 3738 (2537)	Banda, Busoga, Uganda	1972	Human	8
KETRI 3537	Bungoma, Western Province, Kenya	1998	Human	3
KETRI 2656	Lambwe valley,Kenya	1983	Human	2
KETRI 3459	Kitanga, Tanzania	1960	Human	3
EATRO 2291	Busoga, Uganda	1976	Human	1

Molecular Characterization Of Trypanosome Isolates

The parasites (isolates) were originally ascribed as Tbr based on their host identity (human), clinical manifestation and their appearance under microscopy (as trypanosomes). We therefore validated their Tbr species status via PCR. We separately extracted and purified DNA from the individual isolates using Qiagen DNA easy blood and tissue extraction kit (Qiagen, Hilden, Germany) according to the manufacturer's instructions. We then separately performed PCR amplification targeting Tbr species-specific SRA gene[15] in 10∝ l reactions consisting of 2.5 µl DNA, 0.125 units of Taq polymerase (Promega, CA, USA) 1X PCR buffer, 0.2 mM dNTPS, 2 mM $MgCl_2$, 1 ∝M each of forward (SRA A) and reverse (SRA E) primers. The thermocycling conditions included initial step 95^{o}C for 3 min, followed by 35 cycles of 95^{o}C for 30 s, 60^{o}C for 30 s, 72^{O}C for 1 min and final extension at 72^{0}C for 2 min. We included DNA from a validated Tbr as a positive control KETRI 2537 (KETRI 3738)[16] and PCR water as well as T.b.brucei as negative control. We resolved the amplicons on 2% molecular grade Top vision agarose (Thermo Scientific) stained with ethidium bromide, and documented the gel using UVITEC (Cambridge) gel imager.

Experimental Animals

We obtained 145 male Swiss White mice weighing 25–30 g from KALRO-BioRI Small Animals Breeding Unit. The mice were housed in groups of 10 in standard mouse cages and using woodcarvings as bedding material and maintained on a diet consisting of commercial pellets (Unga® Kenya Ltd) and water ad libitum. The mice were kept in a locked room under natural light. Room temperature and humidity were not regulated. We acclimatized the mice to experimental room conditions for two weeks and dewormed them using Noromectin®, Norbrook, UK at 0.2 mg/kg as described by [17] to ensure that they were free of ecto- and endo-parasites. We obtained during this acclimatization period base line data on packed cell volume (PCV) and body weight prior to infection.

Experimental Design

Four (4) donor mice per isolate were immunosuppressed using cyclophosphamide 300 mg/kg for three consecutive days[18] after which the recovered cryopreserved T.b.rhodesiense isolates shown in Table 1were injected for multiplication.The mice were monitored for parasitaemia for 21 days post infection, a period known to be sufficient for development of late stage disease in the mouse model [19]. They were then euthanized using concentrated carbon dioxide (CO_2). At least one mL of heart blood trypanosomes were collected in 5 µl of 10% EDTA enough to prevent coagulation and pooled from the four donor's mice while brain tissues from the four donor mice were also pooled and suspended in cold PSG pH 8.0. Brain tissues were washed in 3 Ml PSG pH 8.0 buffer per wash for at least ten times (total 30Ml PSG buffer) and presence of trypanosomes in every wash carefully examined under the microscope. When no trypanosome could be detected, the final buffer wash was discarded, the brain excised using sharp pair of scissors and gently homogenized in PSG pH 8.0. The supernatant containing brain trypanosomes (CNS) from the four donor mice was pooled. Slide smears of CNS trypanosomes of each of the isolates were made from the brain homogenates. Similarly, smears of BSF trypanosomes from each of the Tbr isolates were made from pooled heart blood. The density of trypanosomes in the pooled supernatant collected from the brain homogenates (Table 3) was then quantified using a haemocytometer. Similarly, the density of the BSF trypanosomes in the pooled heart blood (Table 3) were also quantified and adjusted to the inoculum level of the supernatant containing CNS form trypanosomes using PSG pH 8.0 (Table 3). Either BSF or CNS form of trypanosomes (BSF and CNS) were then intraperitoneally injected into ten experimental mice while five non-infected mice acted as control. The infected mice were monitored for the following parameters: pre-patent period (PP), parasitaemia progression, PCV and body weight once a week, survival, gross pathology, and histopathology. At 30 days post infection, four mice from each group including two non-infected control were sacrificed for gross lesions (lesions and organ weights) and histopathology. The remaining mice were humanly euthanized and disposed.

Pre-patent period (pp) and parasitaemia progression

Blood for estimation of parasitaemia levels was collected daily from each mouse using the tail tip amputation method [20]. The pre-patent period and parasitaemia progression were determined using the rapid matching method [21]. The infected mice were monitored for 30 DPI. The end point of the infected mice was determined by observation of clinical signs such as lethargy and hackle hair, as well as PCV drop of approximately 25% with consistent high parasitaemia levels of 1×10^9/mL − 1 for at least three consecutive days. The animals were sacrificed immediately by CO_2 asphyxiation in accordance with guidelines of the Institutional Animal Care and Use Committee (IUCAC) as described by [22] and recorded as dead animals.

Determination Of Morphology Of Trypanosomes

A drop of blood from mice infected with BSF or CNS derived trypanosomes was collected as infection progressed. Thin smears were then prepared and examined using Leica DM500 microscope at high magnification with oil immersion objective (10 × 100). The length of the trypanosome was measured from the posterior end to the anterior end including the free flagellum as previously outlined by Stephen [23] On average, 50 trypanosomes of BSF or CNS were measured at every time point (DPI) per isolate.

Packed cell volume (PCV) and body weight

These were measured once a week as outlined by Naessens [24] for PCV and by Gitonga [25] for body weight.

Survival

All control mice survived up to the end of the experimental period of 30 days and their survival time data were therefore categorised as censored. The shortest survival time was observed in mice infected with EATRO 2291 at 13.7 ± 2.0 and 12.7 ± 1.5 for BSF or CNS infected mice, respectively (Fig. 7 (v). This was followed by mice infected with KETRI 2656 at 17.6 ± 1.2 and 15.9 ± 0.3 for BSF or CNS infected mice, respectively (Fig. 7 (iii). Mice infected with KETRI 3738, KETRI 3537 and KETRI 3459 survived for period between 26 DPI and end of experiment (Fig. 7 (i), (ii) and (iv)). The p values associated with Wilcoxon and Logrank tests of homogeneity for the BSF or CNS forms of individual isolate ranged between 0.1 to 0.5 and 0.1 to 0.3 respectively showing no significant difference between the groups both at early and longer survival times. However, when the two groups are compared, CNS infected mice survival was shorter compared to BSF infected mice, although not significantly different ($p > 0.05$) (Fig. 7 (vi).

Gross Pathology And Histopathology

Four infected mice from each of the BSF or CNS derived trypanosomes groups including two control mice were sacrificed at 31 DPI for KETRI 3537 and 3738, KETRI 3439 at 29 DPI, EATRO 2291 at 15 DPI and the only surviving mouse of KETRI 2656 at 18 DPI. The body weight of each mouse was determined after which the mouse was euthanized, dissected and the brain, spleen, kidneys, liver, lungs and heart collected and weighed using a weighing balance (Mettler Toledo PB 302 ®, Switzerland). These organs were preserved in 10% formalin and thereafter processed for histopathology as previously described [27]..

Statistical analysis

Analysis was done to test the significant differences between the BSF and CNS forms per isolates in PP, parasitaemia progression, PCV, body weights, trypanosomes length and survival in the two groups. The data obtained from the study were summarized as means ± standard error of mean, while the differences between and within the means were analyzed using one-way ANOVA. The analyses were conducted using

GenStat, UK where $p \leqslant 0.05$ were considered statistically significant. General Linear Model in SAS Release 8.02 was used to analyze data on the length of the trypanosome. Differences between any two means were considered significant at $p < 0.05$. Survival data analysis was carried out employing the Kaplan–Meier method on StatView (SAS Institute, Version 5.0.1) statistical package for determination of survival distribution function. Rank tests of homogeneity were used to determine the effect on host survival time of BSF- and CNS-infected mice [29].

Results

Molecular identification of cryo-bank isolates

The 460 bp SRA gene fragment was amplified confirming all the isolates as T. b. rhodesiense isolates. Our PCR amplification of the 460 bp bands SRA gene (Gibson et al, 2002) in all our isolates, confirmed their Tbr species status (Fig. 1).

Pre-patent Period

On average, 50 blood samples of BSF or CNS infected mice were collected within a period of five days post infection for the determination of the pre-patent period. The isolate specific pre-patent period data showed that mice infected with the KETRI 3738 and KETRI 2656 isolates had significantly ($p < 0.01$) longer pp compared to the other three (KETRI 3537, KETRI 3459, and EATRO 2291) isolates (Fig. 2). The shortest PP was recorded in mice infected with the BSF and CNS forms of KETRI 3537 at 4.4 ± 0.16 and 4.0 ± 0 respectively. In mice groups infected with 2/5 isolates, KETRI 3738 and KETRI 2656, there was a marked difference between the PP of BSF and CNS-derived trypanosomes of either isolate (Fig. 2). This difference was also reflected in the overall mean ± SE pre-patent period, which was 5.2 ± 0.3 and 4.7 ± 0.2 for all the mice that were infected with the BSF and CNS-derived trypanosome trypanosomes, respectively ($p < 0.05$)

Progression Of Parasitaemia In Mice

Parasitaemia in mice infected with either the BSF or CNS derived trypanosomes increased rapidly attaining on average first peak parasitaemia of 6.1×10^8 and 6.8×10^8 trypanosomes/mL(anti-log 8.8) of blood for both BSF and CNS derived trypanosomes (Table 2) showing that in general, the parasitaemia patterns were similar. However, the first peak parasitaemia was attained after an average of 7 and 8 days for CNS and BSF trypanosome forms respectively (Table 2), showing that at the initial stages of the infections, the parasitaemia increase in mice infected with CNS derived trypanosomes was consistently faster than those infected with BSF trypanosomes ($p < 0.05$). A noticeable decline in the first peak parasitaemia was observed in a majority of the isolates (Fig. 3). In general, however, the parasitaemia induced by CNS or BSF trypanosome forms remained high with minor fluctuations throughout the infection (Fig. 3).

Table 2

Mean ± SE peak parasitaemia and days to peak parasitaemia in mice infected with both the BSF and CNS trypanosomes.

Isolate ID	BSF (Log values) Peak par.	Days to peak parasitaemia)	CNS (Log values) Peak par.	Days to peak parasitaemia
KETRI 3738	8.2 ± 0.4 (1.6 × 10^8/Ml)	8	8.7 ± 0.1 (5.0 × 10^8/Ml)	7
KETRI 3537	8.9 ± 0.1 (7.9 × 10^8/Ml)	7	8.7 ± 0.1 (5.0 × 10^8/Ml)	6
KETRI 2656	8.5 ± 0.2 (3.2 × 10^8/Ml	9	9 ± 0.03 (1.0 × 10^9/Ml)	9
KETRI 3459	8.9 ± 0.1 (7.9 × 10^8/Ml)	8	8.8 ± 0.04 (6.3 × 10^8/Ml)	8
EATRO 2291	9.0 ± 0.1 (1.0 × 10^9/Ml)	9	8.9 ± 0.05 (7.9 × 10^8/Ml)	8
Mean ± SE	8.76 ± 0.14 (6.1 × 10^8/Ml)	8 ± 0.28	8.83 ± 0.06 (6.8 × 10^8/Ml)	7.4 ± 0.39

BSF and CNS Parasite Morphology and length

Parasite Morphology

Donor Swiss white mice infected Tbr isolates EATRO 2291, 2-KETRI 2656, 3-KETRI 3459, 4-KETRI 3537 and 5- KETRI 3738 were sacrificed at 21 days DPI and the morphology of giemsa stained CNS and BSF trypanosomes compared. In terms of morphology, the stained CNS trypanosomes were predominantly slender forms (Fig. 4(iii)) while BSF trypanosomes were a mixture of short stumpy and intermediate form trypanosomes (Fig. 4).However, when CNS parasitaemia density of all the isolates were compared, KETRI 2656 CNS was relatively higher than the rest (Fig. 4 (iii)). The density of trypanosomes in pooled heart blood was twice greater than trypanosomes in brain supernatant (Table 3). On the stained giemsa slides, there were 2–3 more trypanosomes per field in BSF as compared to corresponding CNS trypanosomes from the same isolate (Fig. 4).

Table 3
Density of BSF and CNS derived trypanosomes/mL at 21 DPI including experimental mice inoculum doses

ISOLATE NO.	BSF	CNS BSF OR CNS MICE INOCULUM DOSE
EATRO 2291	7.0×10^7	1.0×10^5 1.0×10^5
KETRI 3459	8.0×10^8	4.0×10^5 4.0×10^5
KETRI 2656	5.1×10^8	7.0×10^6 7.0×10^6
KETRI 3537	4.0×10^7	1.0×10^5 1.0×10^5
KETRI 3738	$8.5\ 10^7$	1.5×10^5 1.0×10^5

Length of BSF or CNS forms of trypanosomes

The mean length for the BSF trypanosomes ranged between 23 ± 1.7 (KETRI 3738) to 31.1 ± 1.7 (KETRI 3537) micrometers whereas that of CNS trypanosomes ranged between 23.0 ± 2.1 (KETRI 3537) and 31.3 ± 09 (KETRI 2656) micrometers. On average, the mean ± SE length was 26.5 ± 1.2 and 27.1 ± 1.6 micrometers for BSF and CNS forms of trypanosome respectively (0.6 micrometers) longer for CNS than BSF although this difference was not significant at $p > 0.05$. We observed polymorphism of CNS trypanosomes in mouse blood (Fig. 4 vix)

Packed Cell Volume (PCV)

The pre-infection data on PCV was 53.2 ± 0.8 and 53.3 ± 1.0 for BSF and CNS groups respectively. This was similar to the PCV values of 52.9 ± 2.2 recorded for control group. Mice infected with the two forms of trypanosomes recorded a significant ($p < 0.001$) decline in PCV within the first peak parasitaemia when compared with the pre-infection data (Fig. 5 (i)). At 14 DPI, the PCV decline in CNS infected mice ranged from 40.8 ± 1.6 (19% decline) for KETRI 3459 to 35.3 ± 0.5 (33% decline) for KETRI 2291. Similarly, the PCV of BSF infected mice at 14 DPI ranged from 46.1 ± 1.1 (12% decline) for KETRI 2656 to 38.6 ± 1.4 (32% decline) for KETRI 3537 (Fig. 5, ii). After 14 days post infection, the trend of decline and or recovery of PCV was isolate dependent. Overall, the mean (± SE) PCV of CNS infected mice declined from 53.3 ± 1.0 at day 0 to 39.5 ± 1.2 at 14 DPI (26.9%) while BSF infected mice declined from 53.2 ± 0.8 to 41.8 ± 1.5 (21.6%) same period and was marginally significantly ($p < 0.05$) higher for CNS than BSF derived trypanosomes. In contrast, the PCV for non-infected control increased from 52.9 ± 2.2 at day 0 to 54.9 ± 1.1 (3.8%) at 14DPI

Body Weight

The mean ± SE pre-infection data on body weight was 27.6 ± 1.8 and 27.1 ± 1.8 for BSF and CNS groups respectively whereas the non-infected control group weighed 21.6 ± 2.2.

Mice infected with BSF and CNS derived trypanosomes recorded an increase in body weight as infection progressed, an increase that was however, slower than the increase observed in the un-infected control mice (Fig. 6). The mean ± SE body weight at day 0 ranged between 22.4 ± 0.4 (CNS) to 32.5 ± 1.1 (BSF). At 14 DPI, KETRI 2656 BSF infected mice showed the highest increase from 24.3 ± 1.1 (day 0) to 29.5 ± 0.6, equivalent to 21% increase (Fig. 6 (iii)). However, the increase in the non-infected control over the same period was from 21.7 ± 2.2 at day 0 to 27.7 ± 0.8 equivalent to 28% increase compared to the highest increase recorded by KETRI 2656 (21%) infected mice. Thereafter, all the infected mice continued increasing in body weight with the increase ranging between 7% (EATRO 2291 and KETRI 3459 (CNS) (Fig. 6,(iv &v)) and 24% (KETRI 3537 (BSF)) (Fig. 6, (ii)). When compared as groups of infected mice, the increase in body weight was significantly lower ($p < 0.01$) in CNS than in BSF infected mice (Fig. 6 (vi) as infection progressed with days post infection.

Pathology

Gross pathology

At 30 DPI, the surviving mice were euthanized and results showed splenomegaly and hepatomegaly in all animals infected with either the BSF or CNS derived trypanosomes. In BSF infected mice, the spleen and liver samples weighed 1.05 ± 0.15 and 2.60 ± 0.2 respectively whereas in CNS infected mice the weight for the same organs was 1.30 ± 0.18 and 3.10 ± 0.3 respectively. Spleen and livers of the non-infected control mice (Fig. 8 (vi)) weighed 0.24 ± 0.09 and 1.75 ± 0.05 respectively. There were no significant differences in liver and spleen weights of BSF or CNS infected mice. The mean ± SE live weight of BSF and CNS infected mice at the time of euthanize were 29.1 ± 1.0 and 30.1 ± 0.9 respectively (Fig. 8(vi). Irrespective of BSF or CNS trypanosomes, petechiae hemorrhage was observed in the brain of KETRI 3459. Engorged mesenteric blood vessels were observed in KETRI 3537 infected mice. In KETRI 3738 infected mice, there was generalized organ enlargement and hemorrhages. There was no significant ($p > 0.05$) difference in organ weights between BSF and CNS infected mice. However, organ weights were isolate dependent as was demonstrated by some of the following: the brain weight for KETRI 3537 and 3738 infected mice was significantly ($p < 0.01$) heavier for CNS than BSF at 0.45 ± 0.02 and 0.38 ± 0.03 for KETRI 3537 (CNS and BSF respectively) and 0.43 ± 0.01 and 0.39 ± 0.03 for KETRI 3738 (CNS and BSF respectively) (Fig. 8 (i & ii). The weight of the hearts for KETRI 3537 BSF and CNS infected mice were significantly ($p < 0.01$) heavier than that for the other isolates at 0.35 ± 0.01 whereas the heart weight in the other BSF infected mice ranged between 0.15 ± 0.02 (EATRO 2291) to 0.2 ± 0.01 (KETRI 3738). Similarly, the heart weight for the KETRI 3537 CNS infected mice was 0.21 ± 0.02 (Fig. 8 (ii)and the heart weight for the other CNS infected mice ranged between 0.15 ± 0.02 (EATRO 2291) to 0.18 ± 0.02 (KETRI 3738).

Histopathology

For the BSF group, vascular congestion of the heart, lungs, and spleen and were observed. In addition, the lungs from the BSF groups showed marked alveoli wall thickening and Infiltration with lymphocytes (Fig. 9 (A and B)). Myocardium from both the CNS and BSF groups had focal areas of lymphocytic infiltration (Fig. 9G and H)). Focal areas of lymphocytic infiltration and tubular epithelium necrosis were also observed in the kidney tissues from both the CNS and BSF groups (Fig. 9I and J)). The brain tissues from CNS group showed Infiltration of perivascular areas with lymphocytes, and blood vessels congestion while those from the BSF were all normal (Fig. 9E and F)). Furthermore, marked vascular congestion and infiltration of perivascular areas with lymphocytes were observed in the liver tissues from both BSF andCNS groups (Fig. 9C and D)). In general, the leisons were more pronounced in CNS than BSF infected mice (supplementary Table 5)

Discussion

The current study compared the phenotypic characteristic of the CNS derived trypanosomes in comparison with their BSF trypanosomes predecessor in mice using five isolates which were confirmed to be T.b.r. by the presence of the SRA gene as previously described [15]. The main finding of this study was that the phenotypic characteristics were isolate independent although in general, CNS derived trypanosomes were significantly more pathogenic than the BSF trypanosomes.

The pre-patent period was significantly shorter in CNS than in BSF derived trypanosomes. The parasitaemia of CNS-derived trypanosomes also increased at a consistently higher rate, leading to attainment of the first parasitaemia peak within 7 days as compared to 8 days for BSF-derived trypanosomes, indicating a higher virulence of the CNS derived trypanosomes. According to previous studies, isolates with shorter pp and high parasitaemia are considered virulent [30]. However, after the first peak, there was no difference in the parasitaemia, progression suggesting the forms responded similarly to the humoral immune response. The difference observed during the first parasitaemia peak may be attributed to the morphology of the infecting trypanosomes. At 21 DPI, BSF trypanosomes were represented by intermediate and short stumpy (SS) forms, which are non-proliferating and adapted to tsetse infection [31, 32]. In contrast, CNS derived trypanosomes were long and slender as was also reported by Wolburg, [33]. Long-slender (LS) forms have also previously been reported to proliferate actively[32]. With exception of mice infected with KETRI 2656 whose CNS derived trypanosomes parasitaemia density was relatively high when compared with the other isolates, Fig. (4(iii)), our study observed low density of the CNS derived trypanosomes and was in agreement with previous observation [12]. However, this observation was made at 21DPI from the brain of mice initially passaged with BSF derived trypanosomes. Our study however did not quantify at 21 DPI the density of CNS trypanosomes from the brain of mice passaged with CNS derived trypanosomes to determine whether there is any density difference between the two sets of CNS derived trypanosomes (CNS trypanosomes derived from the BSF forms and CNS trypanosomes derived from the CNS forms of trypanosomes).

Results on the PCV showed that mice infected with BSF or CNS derived trypanosomes recorded significant decline confirming previous observations associating anaemia with human infection [34] as well as with experimental human trypanosomiasis using vervet monkeys and mice [35, 36]. However, data generated from our study indicated that the decline was more significant in mice infected with CNS than in BSF derived trypanosomes. This difference could be associated with the high parasitaemia registered by the CNS infected mice during the first peak parasitaemia resulting to a high extracellular destruction of erythrocytes as previously reported [37]. In their study, these authors observed increased red cell destruction in the spleen from the third day of patent parasitaemia. In another study on mechanisms of controlling anemia [38], data showed rapid development of anemia until the peak of the first wave of parasitaemia. Importantly, in the current study, after first peak, parasitaemia remained relatively high with no difference in parasitaemia progression between the BSF and CNS derived trypanosomes groups in the remaining days of infection. During this period, the decline in PCV recorded stability (Fig. 6 (vi)) characteristic of chronic phase anaemia [36].

Our data on body weight changes showed increase in body weight both in infected and non-infected control with days post infection irrespective of isolate form although the increase in the non-infected control was significantly more. However the increase observed with infected mice was in agreement with previous studies with T. congolense or T. brucei trypanosomes [25, 38] and T. evansi trypanosomes[39] infections. Observations by these authors and by us contradicts previous observations showing relationship between decline in body weight and trypanosomiasis infections using ewes and mice laboratory animals [40, 41] suggesting body weight alone as an inappropriate biomarker of pathogenicity. Indeed our results showed a tremendous body weight increase in mice infected with KETRI 2656 which based on its shortest survival time may be classified as very virulent[42]. The increase according to our data was relatively more in mice infected with BSF than CNS derived trypanosomes. It is not clear as to why body weight should increase as infection progressed, but we partly attribute organomegaly particularly seen in the spleen and liver. Indeed, our results showed that at the end of experiment the spleen and liver organs of BSF and CNS infected mice were heavier when compared with the non-infected control. Our findings showed short survival times for mice infected with EATRO 2291 and KETRI 2656 demonstrating the two isolates as the most virulent among isolates used in this study[27, 38].

On the morphological length of both the BSF and CNS derived trypanosomes, our results gave a range of 23 ± 1.7 to 31.1 ± 1.7 for the BSF trypanosomes and 23.0 ± 2.1 to 31.3 ± 09 for CNS derived trypanosomes which was in agreement with previous observation[43]. This was not significantly different although CNS derived trypanosomes measured relatively longer than the BSF trypanosomes. This suggests that the CNS derived trypanosomes maintained a higher density of long and slender forms. This increase in length was observed during the early days of mice infection with CNS derived trypanosomes and was maintained throughout the infection period. Whether this difference in length resulted in the difference observed in pathology between the two forms will require further investigations.

Splenomegaly and hepatomegaly have been reported in experimental human African trypanosomiasis using animals[44] and also in humans [45] as some of the symptoms associated with the haemolyphatic

stage of infection [46, 47]. Results from our study confirmed this observation in both BSF and CNS derived trypanosomes infected mice although these symptoms were more pronounced in the CNS than in BSF trypanosomes infected mice. In a previous study, splenomegaly was associated with the acute and post-acute phase of Trypanosoma lewisi infections of laboratory rats [48] and this may be attributed to the proliferation of Lymphocytes according Benoit [49]. Stijlemans[50], attributed hepatosplenomegaly to an enhanced extramedullary erythropoiesis occurring mainly in the spleen and to a lesser extent in the liver. The difference we observed in our study could be attributed to the severity of CNS over BSF infected mice. In a study by Muchiri [51], the authors observed pronounced splenomegaly and hepatomegaly in T.b. rhodesiense isolates causing severe as compared to those causing less severe infection.

The present study recorded tissue inflammation in mice infected with the two forms and was in consistent with previous observations [27, 51]. Trypanosome-induced inflammation lesions were more intense in CNS than in BSF derived trypanosomes infected mice which could be informed by the enhanced tissue invasion in CNS infected mice. Indeed, results from the present study showed higher density in the brain of mice infected with KETRI 2656 CNS trypanosomes.

Conclusion

The phenotypic characteristics of CNS derived-trypanosomes are poorly understood. To investigate these characteristics, we compared morphologic and phenotypic characteristics associated with BSF and CNS derived trypanosomes directly harvested from the blood and the brain, respectively, and evaluated their pathogenicity. our results have demonstrated that CNS derived trypanosomes are relatively more pathogenic than BSF forms when measured in terms of pre-patent period, parasitaemia development, PCV and organ pathology. It is possible that the parasitaemia proliferation within the first peak influences the pathological response considering that in this study, CNS trypanosomes proliferated at a higher rate than the BSF trypanosomes during the first peak parasitaemia. We further identified KETRI 2656 as a suitable isolate for acute menigo- encephalitic studies. We recommend further studies to determine the factors influencing the observed variation in pathogenicity between the CNS and BSF forms.

Abbreviations

CNS	Central Nervous system
BSF	Blood stream forms
Tbr	Trypanosoma brucei rhodesiense
KETRI	Kenya Trypanosomiasis Research Institute
EATRO	East Africa Trypanosomiasis Research Organization
PP	Pre-patent period
PCV	Packed Cell Volume
LS	Long slender
DPI	Days post infection
HAT	Human African trypanosomiasis
BioRI	Biotechnology Research Institute
KALRO	Kenya Agricultural and Livestock Research Organization
IACUC	Institutional Animal Care and Use Committee
DNA	deoxyribonucleic acid
PCR	Polymerase chain reaction
SRA	Serum resistant gene
EDTA	Ethylenediamine tetraacetic acid
PSG	Phosphate saline glucose
BBB	Blood brain barrier

Declarations

Ethics approval and consent to participate

All protocols and procedures used in this study involving laboratory animals were reviewed and approved by the Institutional Animal Care and Use Committee of KALRO-BioRI (protocol number C/BioRI/4/325/11/49).

Consent for publication

Not applicable

Availability of data and material

The datasets during and/or analyzed during the current study are available from the corresponding author on reasonable request.

Competing interests

The authors declare that they have no competing interests

Funding

This study received funding from the Kenya Government through Kenya Agricultural and Livestock research organization (KALRO). All the authors except two, John Thuita and Paul Okumu are employee of KALRO. The Organization was involved in the design of the study, data collection, and analysis, interpretation of data and in writing the manuscript.

Authors Contribution;

KN Developed the proposal, conducted the study and prepared the draft manuscript.

GAM Reviewed the proposal, supervised and reviewed every part of the manuscript development as well sourcing of funds.

JKT Assisted in proposal development, supervision of the study and in the preparation of the draft manuscript.

JMK Reviewed the manuscript and assisted in the preparation of the draft manuscript.

POM. Assisted in the manuscripts drafting and reviewing.

GNN. Statistical analysis of the entire data, interpretation and manuscript development

PKG. Handled the experimental animals, assisted in infecting the experimental animals, data collection and recording

SOG Performed the molecular analysis and interpreted the results

JEA Assisted in the proposal writing, supervised the entire study and in drafting the manuscript.

POO Supervised the processing of histology tissues, read and interpreted histological slides and assisted in manuscript development.

REM. The key Supervisor of the entire study from proposal development to manuscript development

All authors read and approved the final manuscript

Acknowledgements

We acknowledge the Director, KALRO for permission to publish this study. Our other acknowledgment goes to Dr. Sylvance Okoth, former Director BioRi for resources and facilitation, technical staff of Lab three of KALRO- BioRI and in particular Stephen Mbugua for assisting in collection of histological tissues ,John Ndichu and Jane Hanya for taking care of the infected mice.

References

1. Franco JR, Simarro PP, Diarra A, Jannin JG. Epidemiology of human African trypanosomiasisClin Epidemiol. 2014;6:257-75; doi: 10.2147/CLEP.S39728.
2. Brun R, Blum J, Chappuis F, Burri C. Human African trypanosomiasis. Lancet. 2010;375 9709:148-59; doi: 1016/S0140-6736(09)60829-1.
3. Kuepfer I, Hhary EP, Allan M, Edielu A, Burri C, Blum JA. Clinical Presentation of T.b. rhodesiense Sleeping Sickness in Second Stage Patients from Tanzania and Uganda PLoS Negl Trop Dis. 2011;5 3:e968.
4. Greenwood B, Whittle H. The pathogenesis of sleeping sickness.. Trans R Soc Trop Med Hyg. 1980;74 6:716-25.
5. Masocha W, Kristensson K. Passage of parasites across the blood-brain barrier. Virulence. 2012;3 2:202-12; doi: 10.4161/viru.19178.
6. Atouguia JLM, Kennedy PGE (eds.): Neurological aspects of human African trypanosomiasis. Oxford: Butterworth-Heinemann.; 2000.
7. Rodgers J, Bradley B, Kennedy PGE. Delineating neuroinflammation, parasite CNS invasion, and blood-brain barrier dysfunction in an experimental murine model of human African trypanosomiasis. Methods. 2017;127:79-87; doi: 1016/j.ymeth.2017.06.015.
8. Laperchia C, Palomba M, Etet PFS, Rodgers J, Bradley B, Montague P, et al. Trypanosoma brucei Invasion and T-Cell Infiltration of the Brain Parenchyma in Experimental Sleeping Sickness: Timing and Correlation with Functional Changes. PLoS Negl Trop Dis 2016;10 12:e0005242; doi: 1371/journal.pntd.0005242.
9. Lentner C (ed.) Units of Measurement, Body Fluids, Composition of the Body**, Nutrition**. Basel, Switzerland1981.
10. Wolburg H, Mogk S, Acker S, Frey C, Meinert M, Schönfeld C, et al. Late Stage Infection in Sleeping Sickness. PLoS One. 2012;7 3:e34304; doi: 1371/journal.pone.0034304
11. Pentreath V (ed.) Cytokines and the blood-brain barrier in human and experimental African trypanosomiasis. Paris: Springer; 1999.
12. Mogk S, Meiwes A, Shtopel S, Schraermeyer U, Lazarus M, Kubata B, et al. Cyclical Appearance of African Trypanosomes in the Cerebrospinal Fluid: New Insights in How Trypanosomes Enter the CNS. PLoS ONE. 2014;9 3:e91372; doi: org/10.1371/journal.pone.0091372.
13. Lamour SD, Alibu VP, Holmes E, Sternberg JM. Metabolic Profiling of Central Nervous System Disease in Trypanosoma brucei rhodesiense Infection. J Infect Dis. 2017;216 10:1273-80; doi:

10.1093/infdis/jix466

14. Murilla GA, Ndung'u K, Thuita JK, Gitonga PK, Kahiga DT, Auma JE, et al. Kenya Trypanosomiasis Research Institute Cryobank for Human and Animal Trypanosome Isolates to Support Research: Opportunities and Challenges. PLoS Negl Trop Dis. 2014;8 5:e2747; doi: org/10.1371/journal.pntd.0002747.
15. Gibson W, Backhouse T, Griffiths A. The human serum resistance associated gene is ubiquitous and conserved in Trypanosoma brucei rhodesiense throughout East Africa. Infect Genet Evol. 2002;1 3:207-14.
16. Gathogo M, Mukiria P, JohnThuita, Adunga V, Guya S, Wanjiru R, et al. Molecular Identification of African Trypanosome Stabilates from Livestock in Lamu County, Kenya. Journal of Natural Sciences Research. 2017;7 10.
17. Ash LS, Oliver, James H. Susceptibility of Ornithodoros parkeri (Cooley) (Acari: Argasidae) and Dermanyssus gallinae (DeGeer) (Acari: Dermanyssidae) to Ivermectin. Journal of Medical Entomology. 1989;26:133-9(7).
18. Wombou Toukam C, Solano P, Bengaly Z, Jamonneau V, Bucheton B. Experimentalevaluation of xenodiagnosis to detect trypanosomes at low parasitaemia levels in infected hosts. parasite Immunol. 2011;18:295-302.
19. Jennings F, Whitelaw D, Urquhart G. The relationship between duration of infection with Trypanosoma brucei in mice and the efficacy of chemotherapy. Parasitology. 1977;75 2:143-53.
20. Saito MS, Lourenço AL, Kang HC, Rodrigues CR, Cabral LM, Castro HC, et al. New approaches in tail-bleeding assay in mice: improving an important method for designing new antithrombotic agents. Int J Exp Pathol. 2016;97 3:285-92; doi: 10.1111/iep.12182
21. Herbert WJ, and Lumsden WH. Trypanosoma brucei: A rapid “matching” method for estimating the host parasitaemia. Experimental Parasitology. 1976;40:427-31.
22. Martinez-Gutierrez M, Correa-Londoño L, Castellanos J, Gallego-Gómez J, Osorio J. Lovastatin Delays Infection and Increases Survival Rates in AG129 Mice Infected with Dengue Virus Serotype 2. PLoS ONE. 2014;9 2:e87412; doi: org/10.1371/journal.pone.0087412.
23. Stephen L (ed.) Trypanosomiasis: A Veterinary Perspective. New York1986.
24. Naessens J, Kitani H, Nakamura Y, Yagi Y, Sekikawa K, Iraqi F. TNF-a mediates the development of anaemia in murine *Trypanosoma brucei brucei* infection, but not the anaemia associated with murine *Trypanosoma congolense* infection. Clin Exp Immunol. 2005;139 3:405-10.
25. Gitonga PK, Ndung’u K, Murilla GA, Thande PC, Wamwiri FN, Auma JE, et al. Differential virulence and tsetse fly transmissibility of Trypanosoma congolense and Trypanosoma brucei strains. Onderstepoort J Vet Res. 2017;84 1:1412; doi: 10.4102/ojvr.v84i1.1412.
26. Subramaniam KS, Datta K, Marks MS, Pirofski L-a. Improved Survival of Mice Deficient in Secretory Immunoglobulin M following Systemic Infection with Cryptococcus neoformans. Infect Immun. 2010;78 1:441-52; doi: 10.1128/IAI.00506-09

27. Kariuki C, Kagira J, Mwadime V, Ngotho M. Virulence and pathogenicity of three Trypanosoma brucei rhodesiense stabilates in a Swiss white mouse model. Afr J Lab Med. 2015;4 1:137; doi: org/10.4102/ajlm.v4i1.137.
28. Katherine N. Gibson-Corley, Alicia K. Olivier, Meyerholz DK. Principles for valid histopathologic scoring in research. Vet Pathol. 2013;50 6; doi: 10.1177/0300985813485099.
29. Everitt BS, Der G (eds.): A Handbook of Statistical Analysis Using SAS. London, New York, Washington D. C.1998.
30. Morrison L. Parasite-driven pathogenesis in Trypanosoma brucei infections. Parasite Immunol. 2011;33 8:448-55; doi: 10.1111/j.1365-3024.2011.01286.x.
31. Silvester E, McWilliam KR, Matthews KR. The Cytological Events and Molecular Control of Life Cycle Development of Trypanosoma brucei in the Mammalian Bloodstream. Pathogens. 2017;6 3:29; doi: 10.3390/pathogens6030029.
32. Rico E, Rojas F, Mony BM, Szoor B, MacGregor P, Matthews KR. Bloodstream form pre-adaptation to the tsetse fly in Trypanosoma brucei.Front Cell Infect Microbiol. 2013;3 78; doi: 10.3389/fcimb.2013.00078.
33. Wolburg H, Mogk S, Acker S, Frey C, Meinert M, Schönfeld C, et al. Late Stage Infection in Sleeping Sickness. PLoS One. 2012;7 3:e34304; doi: 10.1371/journal.pone.0034304.
34. Chisi J, Misiri H, Zverev Y, Nkhoma A, Sternberg J. Anaemia in human African trypanosomiasis caused by Trypanosoma brucei rhodesiense. East Afr Med J. 2004;81 10:505-8.
35. Thuita JK, Kagira JM, Mwangangi D, Matovu E, Turner CMR, Masiga. D. Trypanosoma brucei rhodesiense Transmitted by a Single Tsetse Fly Bite in Vervet Monkeys as a Model of Human African Trypanosomiasis. PLoS Negl Trop Dis. 2008;2 5:e238; doi: 10.1371/journal.pntd.0000238.
36. Amole BO, Clarkson AB, Jr, Shear HL. Pathogenesis of anemia in Trypanosoma brucei-infected mice. Infect Immun. 1982 36 3:1060-8.
37. Ikede B, Lule M, Terry R. Anaemia in trypanosomiasis: mechanisms of erythrocyte destruction in mice infected with Trypanosoma congolense or T. brucei. Acta Trop. 1977;34 1:53-60.
38. Noyes HA, Alimohammadian MH, Agaba M, Brass A, Fuchs H, Gailus-Durner V, et al. Mechanisms Controlling Anaemia in Trypanosoma congolense Infected Mice. PLoS One. 2009;4 4:e5170; doi: 10.1371/journal.pone.0005170.
39. Kamidi C, Auma J, Mireji P, Ndungu K, Bateta R, Kurgat R, et al. Differential virulence of camel Trypanosoma evansi isolates in mice. Parasitology. 2018:1-8; doi: org/10.1017/S0031182017002359.
40. Edeghere H, Elhassan E, Abenga J, Osue H, Lawani F, Falope O. Effects of infection with Trypanosoma brucei brucei on different trimesters of pregnancy in ewes.. Vet Parasitol. 1992;43 3-4:203-9.
41. Trindade S, Rijo-Ferreira F, Carvalho T, Pinto-Neves D, Guegan F, Aresta-Branco F, et al. Adipose tissue is a major reservoir of functionally distinct trypanosoma brucei parasites. American Journal of Tropical Medicine and Hygiene. 2017;95 5:606-.

42. Masumu J, Marcotty T, Geysen D, Geerts S, Vercruysse J, Dorny P, et al. Comparison of the virulence of Trypanosoma congolense strains isolated from cattle in a trypanosomiasis endemic area of eastern Zambia. Int J Parasitol. 2006;36 4:497-501.
43. Büscher P, Cecchi G, Jamonneau V. Human African trypanosomiasis. Lancet. 2017;390:2397-409; doi: 10.1016/S0140-6736(17)31510-6.
44. Morrison L, Tait A, McLellan S, Sweeney L, Turner C, MacLeod A. A Major Genetic Locus in Trypanosoma brucei Is a Determinant of Host Pathology. PLoS Negl Trop Dis. 2009;3 12:e557; doi: org/10.1371/journal.pntd.0000557.
45. Malvy D, Chappuis F. Human African trypanosomiasis, review, sleeping sickness,Trypanosoma brucei gambiense ,Trypanosoma brucei rhodesiense , tsetse Article. Clin Microbiol Infect. 2011;17:986-95.
46. MacLean L, Odiit M, Chisi J, Kennedy P, Sternberg J. Focus-Specific Clinical Profiles in Human African Trypanosomiasis Caused by Trypanosoma brucei rhodesiense. PLoS Negl Trop Dis. 2010; 4 12:e906; doi: org/10.1371/journal.pntd.0000906.
47. Vincendeaul P, Bouteillell B. Immunology and immunopathology of African trypanosomiasis. An Acad Bras Ciênc. 2006;78 4; doi: org/10.1590/S0001-37652006000400004
48. Thoongsuwan S, Cox H. Anemia, splenomegaly, and glomerulonephritis associated with autoantibody in Trypanosoma lewisi infections. J Parasitol. 1978;64 4:669-73.
49. Robinett JP, Rank RG. Splenomegaly in Murine Trypanosomiasis: T Cell-Dependent Phenomenon. Infection and Immunity. 1979;23 2:270-5.
50. Stijlemans B, Baetselier PD, Magez S, Ginderachter JAV, Trez CD. African Trypanosomiasis-Associated Anemia: The Contribution of the Interplay between Parasites and the Mononuclear Phagocyte System. Front Immunol. 2018; doi: org/10.3389/fimmu.2018.00218.
51. Muchiri MW, Ndung'u K, Kibugu JK, Thuita JK, Gitonga PK, Ngae GN, et al. Comparative pathogenicity of Trypanosoma brucei rhodesiense in Swiss White mice and Mastomys natalensis rats. Acta Tropica. 2015;150:23-8.

Figures

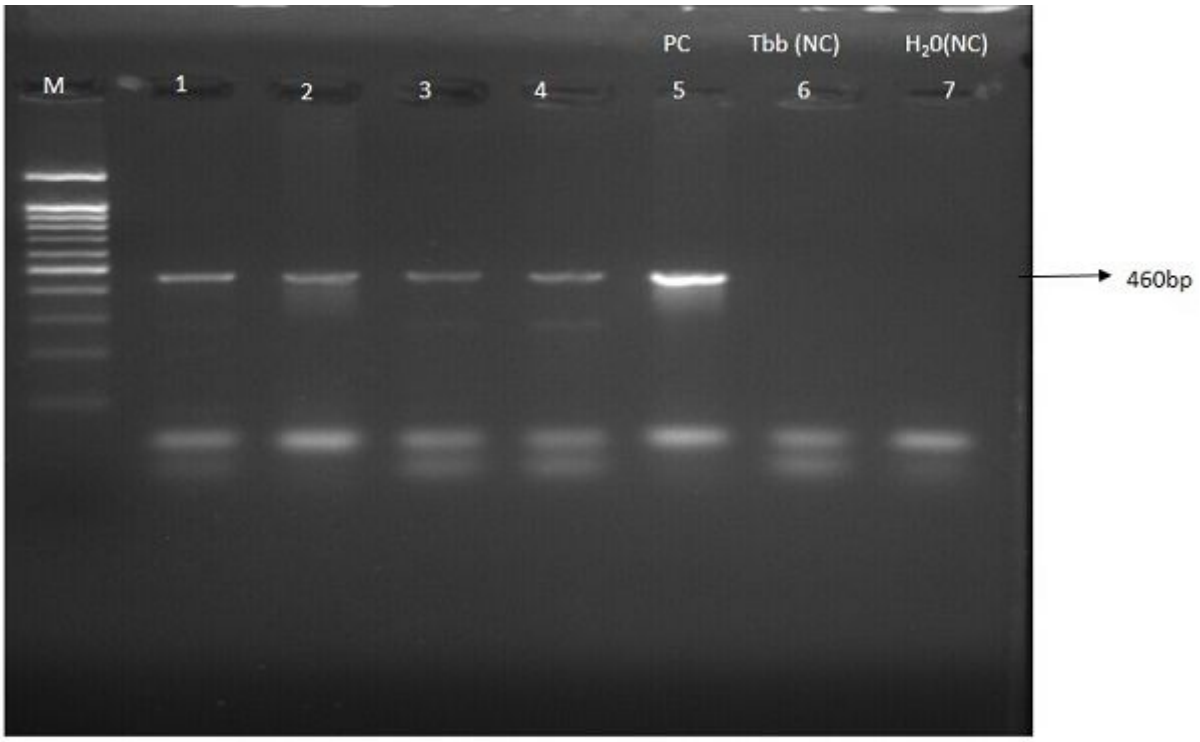

Figure 1: M=marker;1=KETRI 3537;2=KETRI 2656;3=KETRI 3459;4=EATRO 2291; 5=KETRI 3738; PC=Positive control; 6=*Trypanosoma brucei brucei*-Negative control (NC) and 7=Water-Negative control(NC)

Figure 1

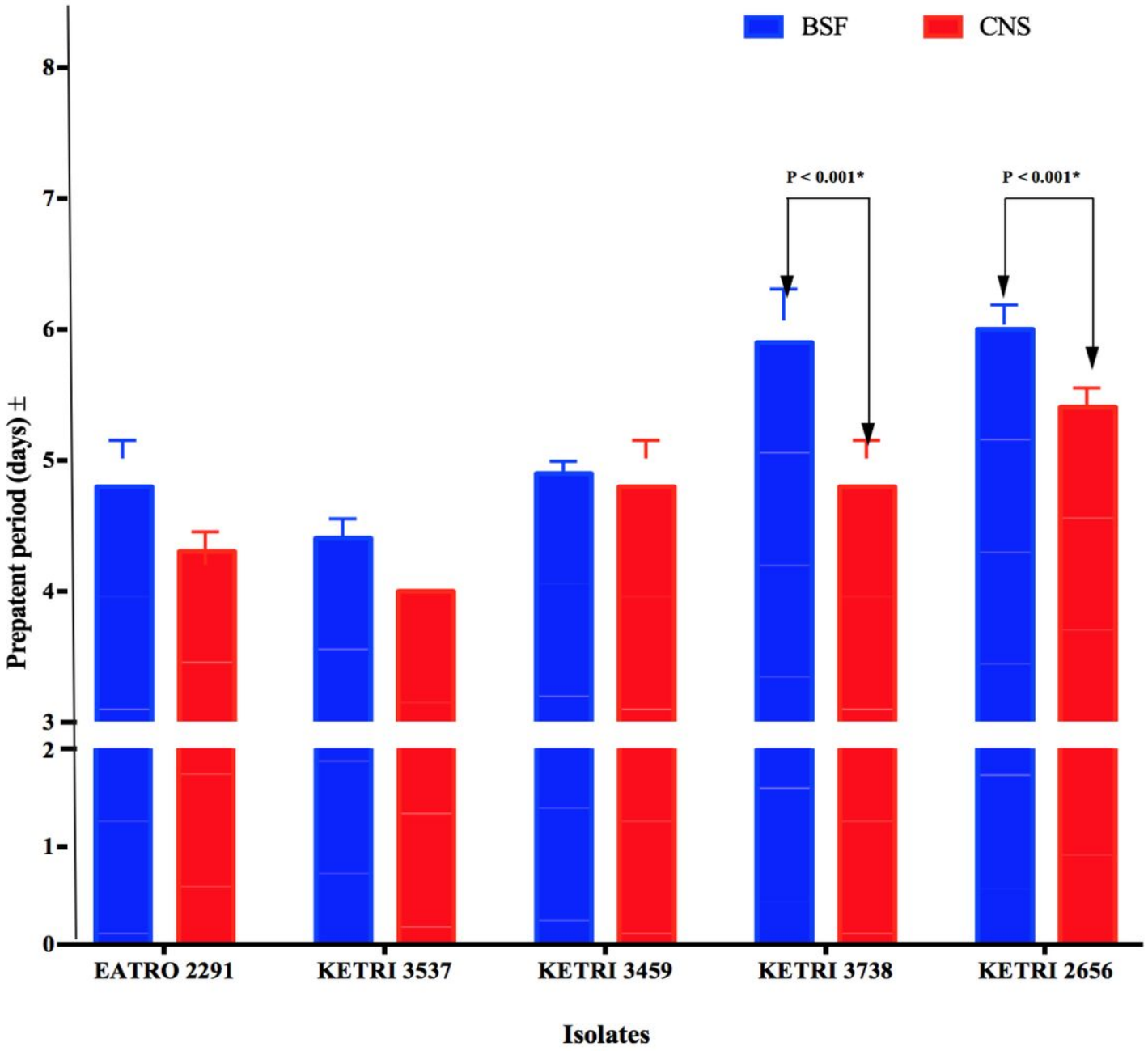

Figure 2. Pre-patent in mice infected with BSF or CNS trypanosomes

Figure 2

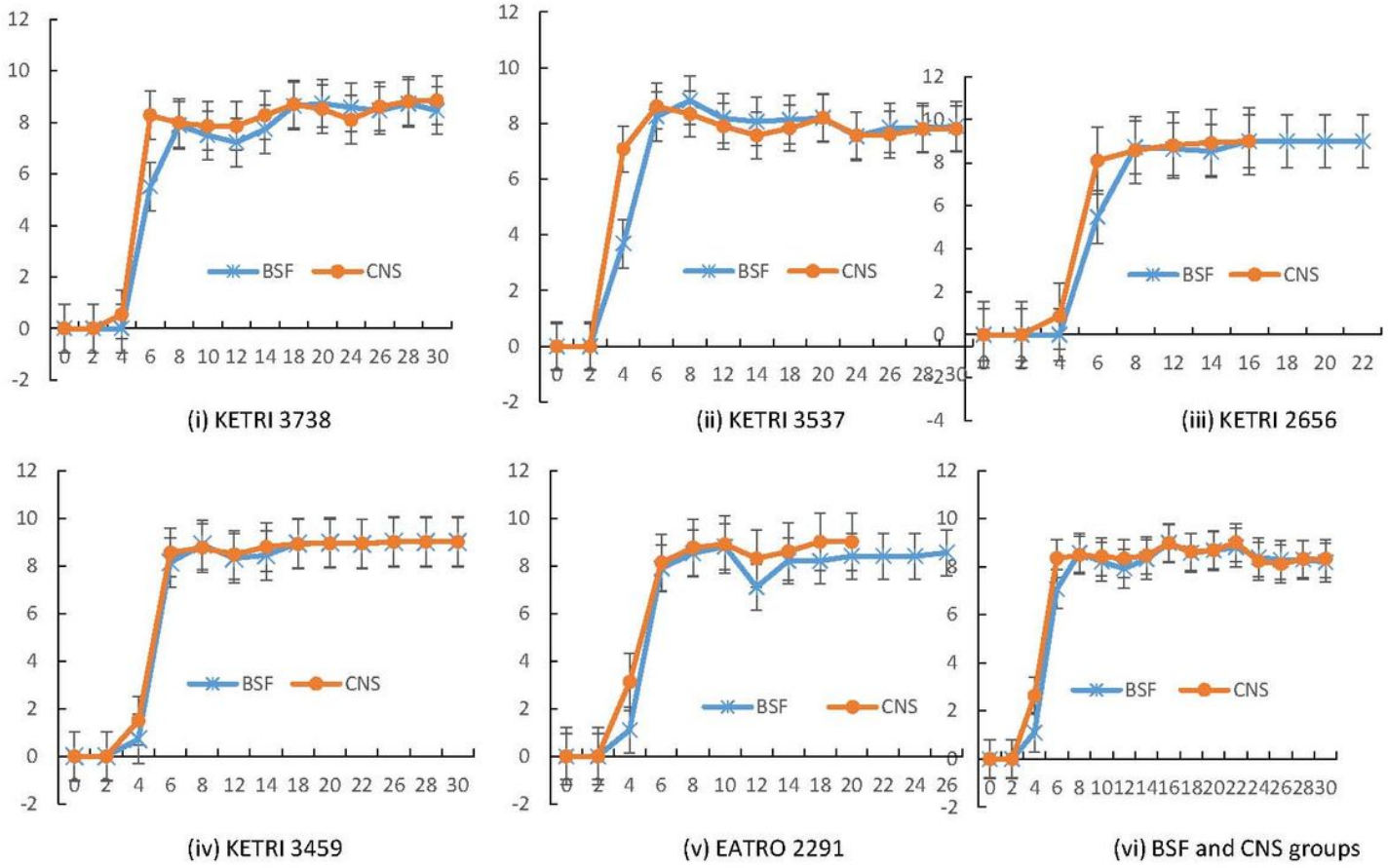

Figure 3 Parasitaemia progression in mice infected with *Trypanosoma b. rhodesiense* BSF or CNS forms

Figure 3

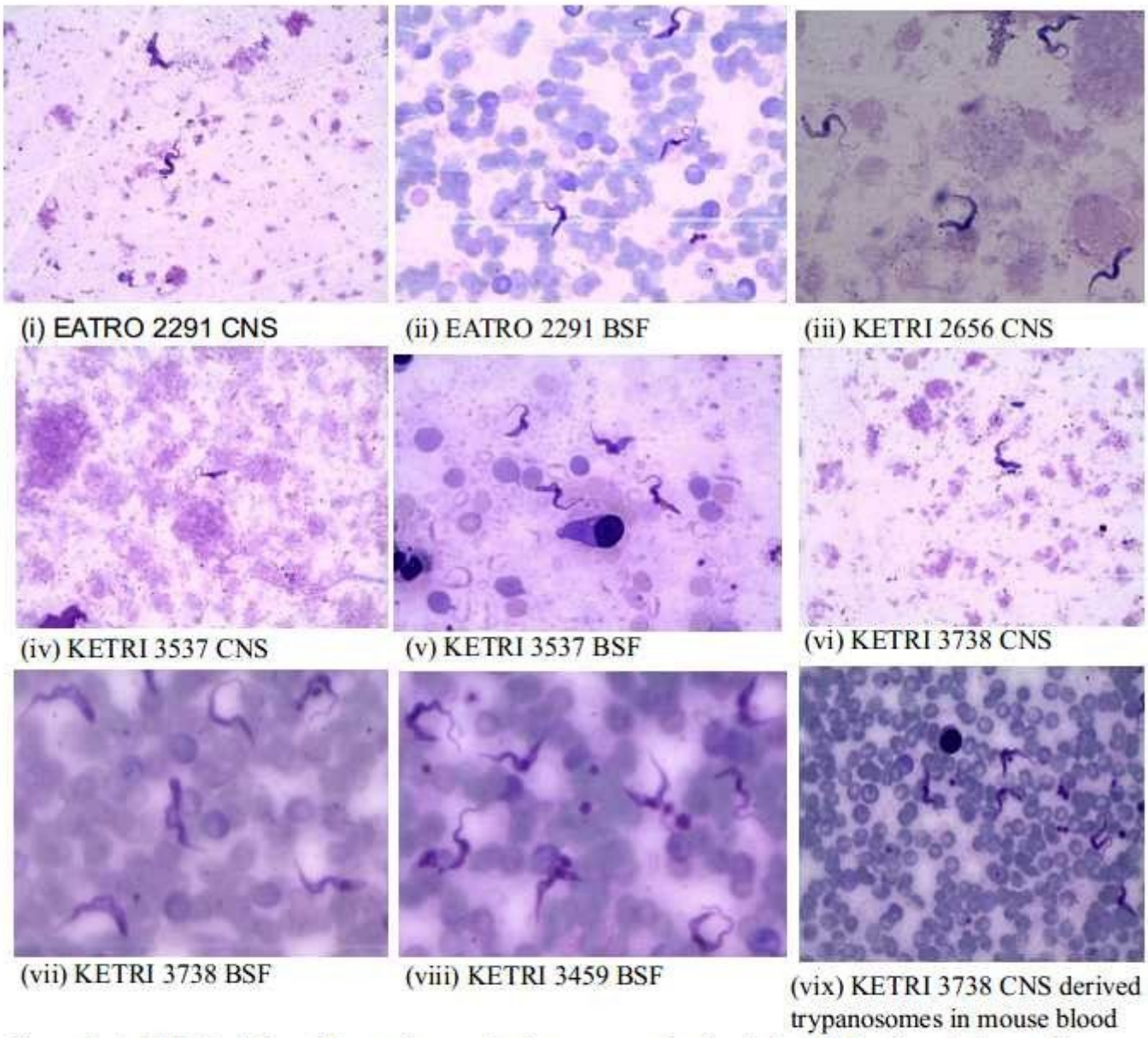

Figure 4 At 21 DPI, infected four mice per isolate were euthanized, heart blood pooled as well as the brain tissue, homogenized and thin smears for morphological characteristics made from pooled heart blood and pooled homogenized brain tissue. Slides were examined at 10x100 magnification using the oil immersion objective. Figure (vix) shows polymorphism of CNS trypanosomes in mouse blood.

Figure 4

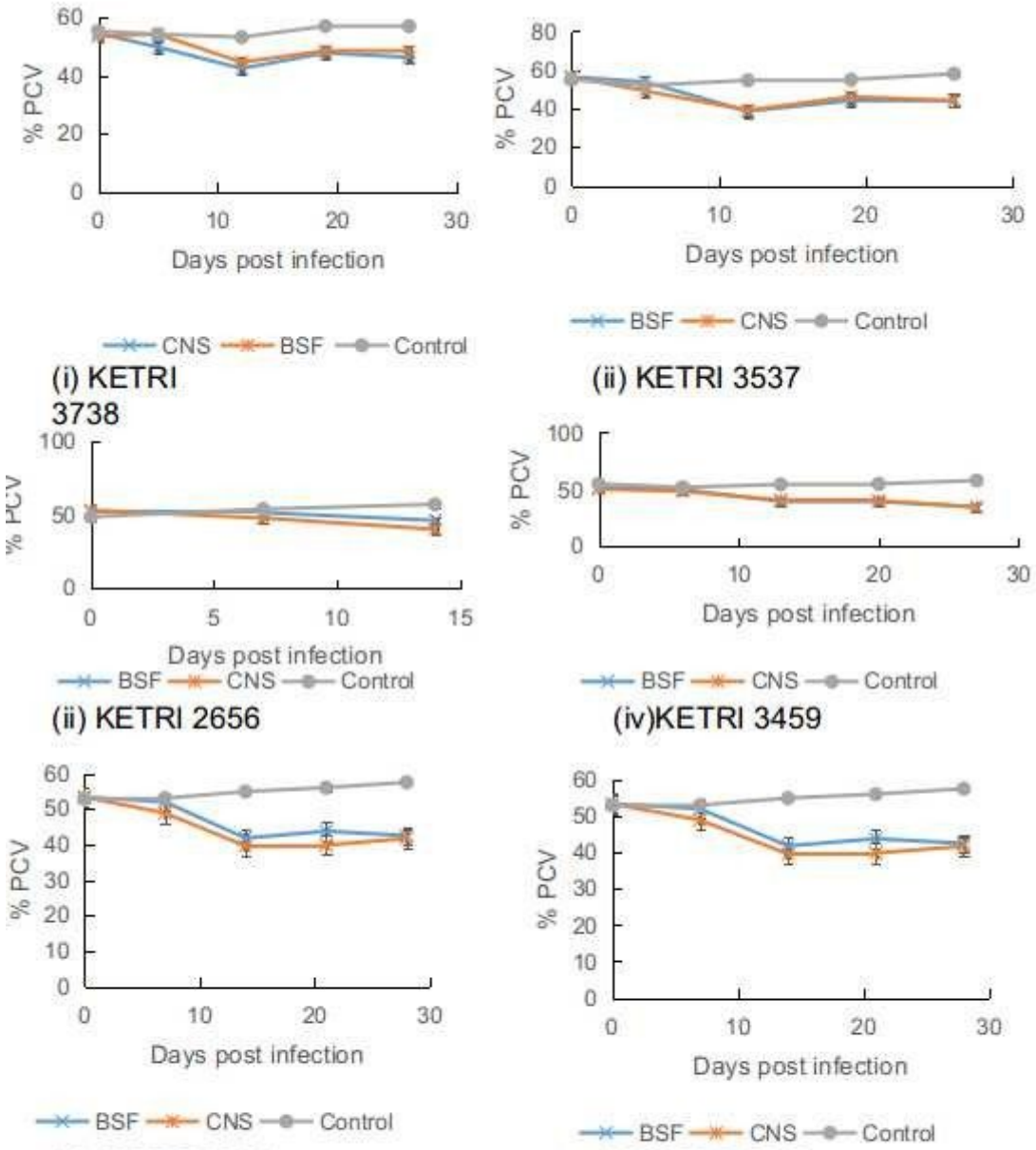

Fig 5 PCV changes in mice infected with BSF and CNS derived trypanosomes

Figure 5

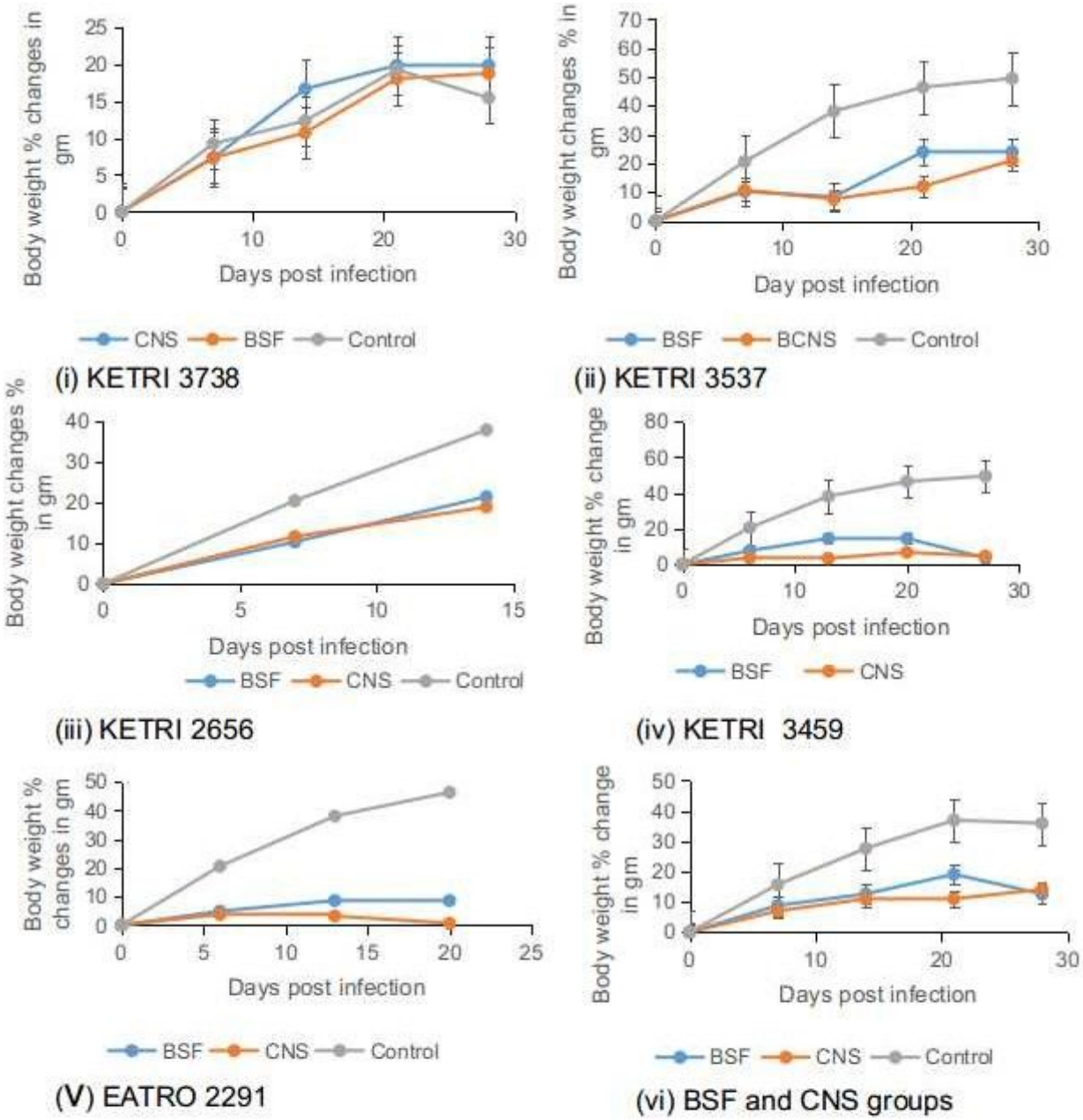

Fig 6: Body weight changes in days post infection expressed in % from day 0 in mice infected with BSF or CNS derived trypanosomes.

Figure 6

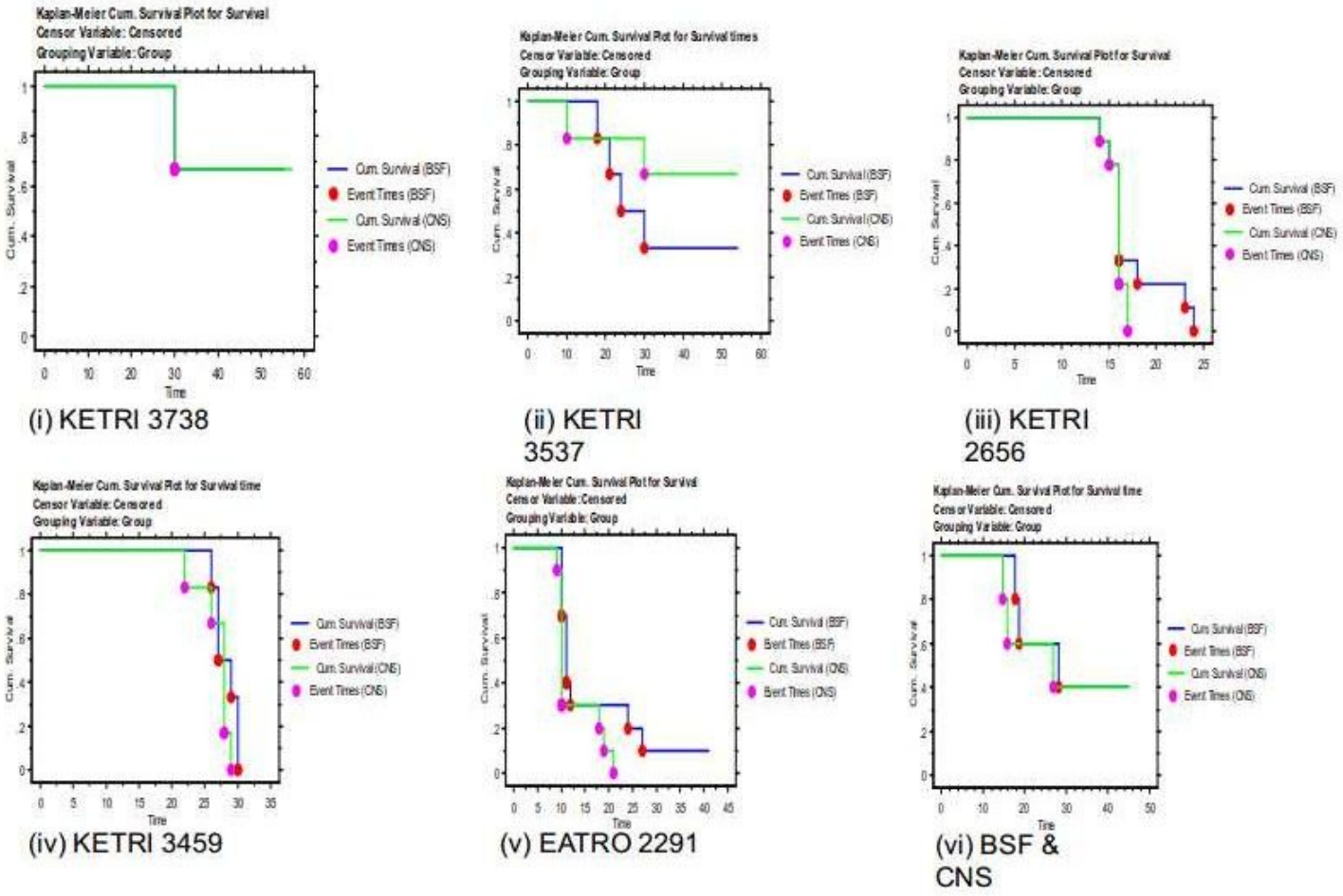

Fig 7 Mean ±Se of mice survival (n=6); BSF, blood stream forms, CNS, central nervous system forms :(i) KETRI 3738, (ii) KETRI 3537, (iii) KETRI 2656, (iv) KETRI 3459, (v) EATRO 2291 and (vi) BSF and CNS infected mice grouped together.

Figure 7

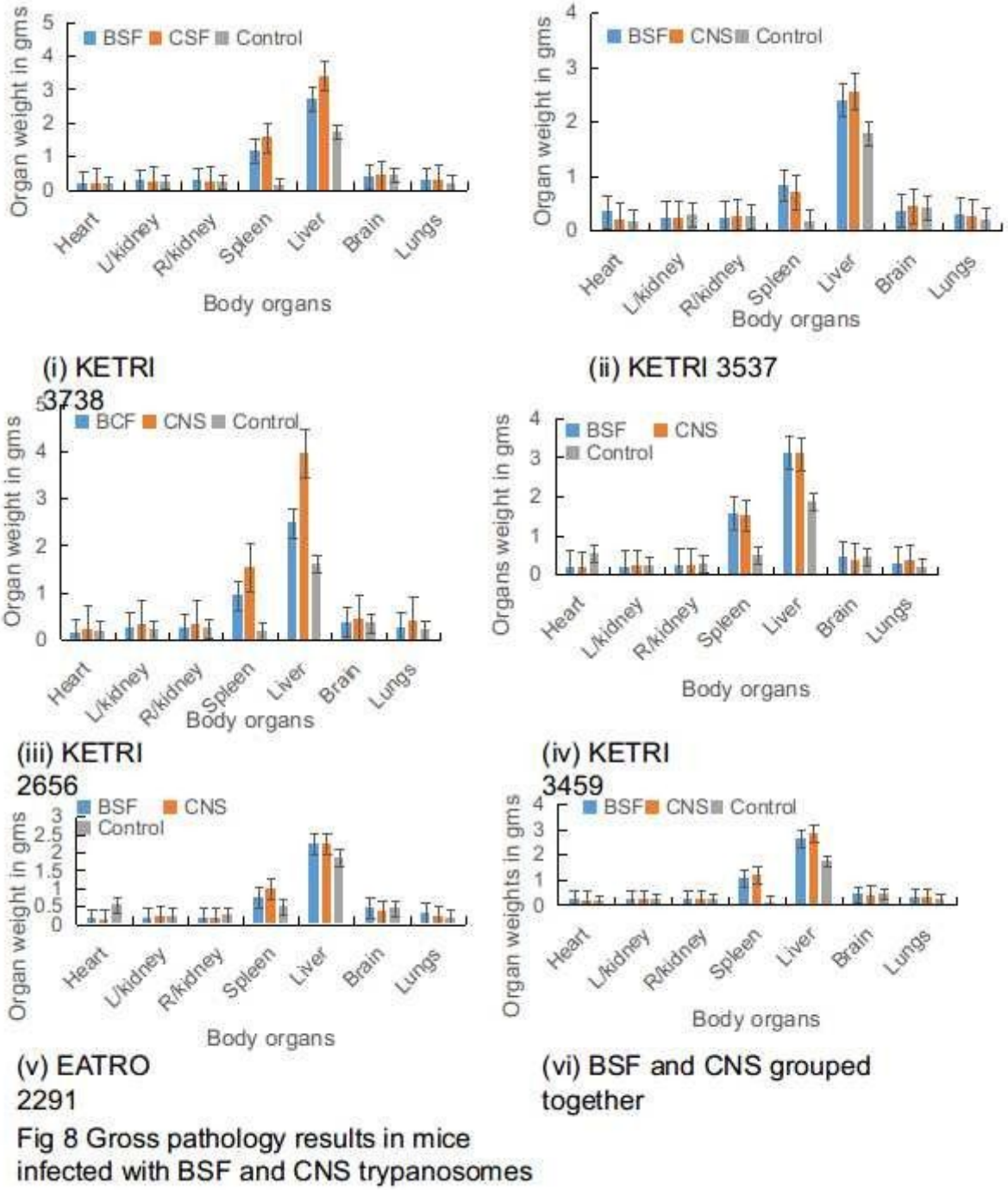

Fig 8 Gross pathology results in mice infected with BSF and CNS trypanosomes

Figure 8

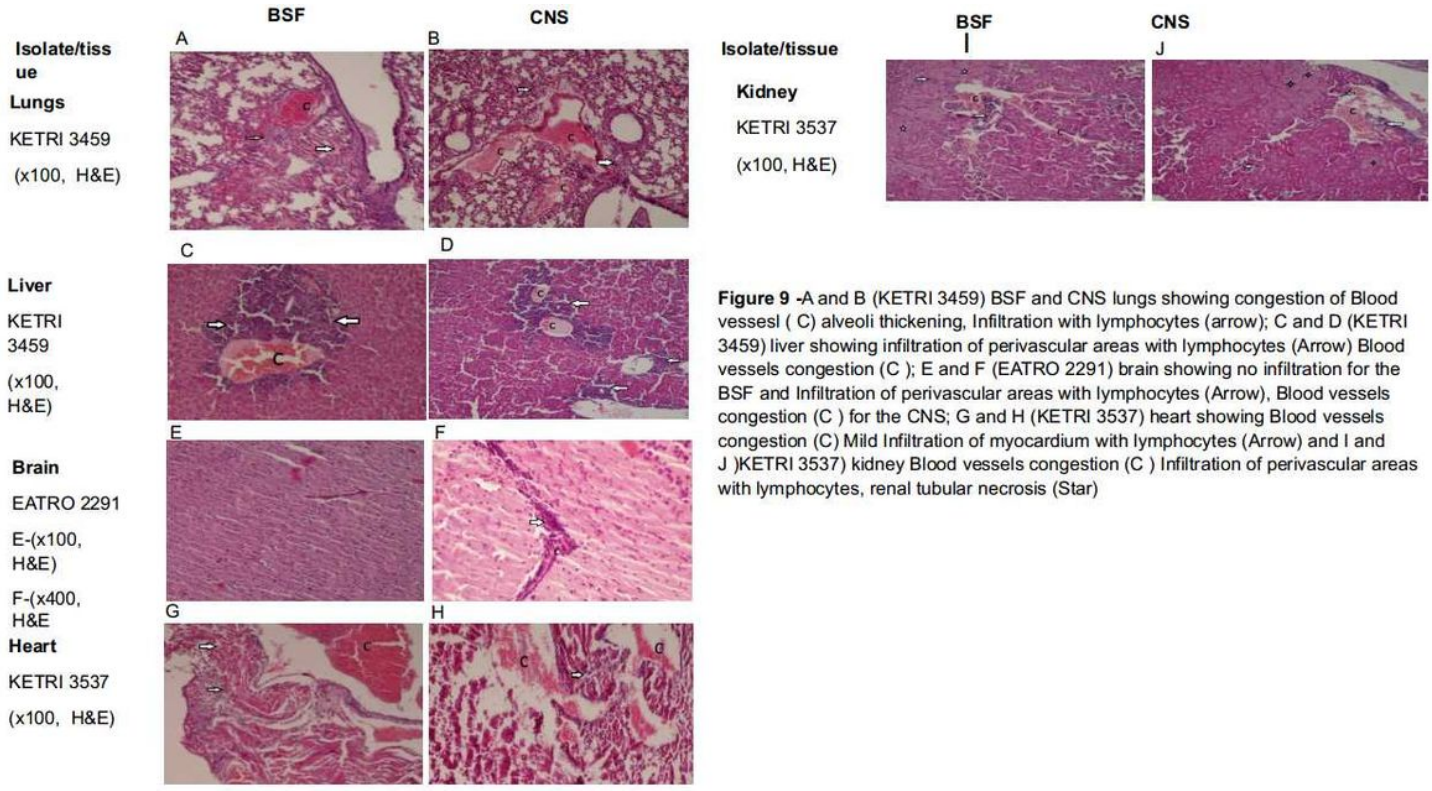

Figure 9 -A and B (KETRI 3459) BSF and CNS lungs showing congestion of Blood vessesl (C) alveoli thickening, Infiltration with lymphocytes (arrow); C and D (KETRI 3459) liver showing infiltration of perivascular areas with lymphocytes (Arrow) Blood vessels congestion (C); E and F (EATRO 2291) brain showing no infiltration for the BSF and Infiltration of perivascular areas with lymphocytes (Arrow), Blood vessels congestion (C) for the CNS; G and H (KETRI 3537) heart showing Blood vessels congestion (C) Mild Infiltration of myocardium with lymphocytes (Arrow) and I and J)KETRI 3537) kidney Blood vessels congestion (C) Infiltration of perivascular areas with lymphocytes, renal tubular necrosis (Star)

Figure 9

Supplementary Files

This is a list of supplementary files associated with this preprint. Click to download.

- Graphicalabstract.jpg
- SupplementaryTable5.docx